Crystal structure of $Ca_{12}Al_{14}O_{32}Cl_2$ and luminescence properties of $Ca_{12}Al_{14}O_{32}Cl_2$:Eu^{2+}

Tomoyuki Iwata, Masahide Haniuda, Koichiro Fukuda*

Department of Environmental and Materials Engineering, Nagoya Institute of Technology, Nagoya 466-8555, Japan

Abstract

The crystal structure of $Ca_{12}Al_{14}O_{32}Cl_2$ was determined from laboratory X-ray powder diffraction data ($CuK\alpha_1$) using the Rietveld method, with the anisotropic displacement parameters being assigned for all atoms. The crystal structure is cubic (space group $I\bar{4}3d$, $Z = 2$) with lattice dimensions $a = 1.200950(5)$ nm and $V = 1.73211(1)$ nm^3. The reliability indices calculated from the Rietveld method were $R_{wp} = 8.48\%$ ($S = 1.21$), $R_p = 6.05\%$, $R_B = 1.27\%$ and $R_F = 1.01\%$. The validity of the structural model was verified by the three-dimensional electron density distribution, the structural bias of which was reduced as much as possible using the maximum-entropy methods-based pattern fitting (MPF). The reliability indices calculated from the MPF were $R_B = 0.75\%$ and $R_F = 0.56\%$. In the structural model there are one Ca site, two Al sites, two O sites and one Cl site. This compound is isomorphous with $Ca_{12}Al_{10.6}Si_{3.4}O_{32}Cl_{5.4}$. Europium-doped sample $Ca_{12}Al_{14}O_{32}Cl_2$:Eu^{2+} was prepared and the photoluminescence properties were presented. The excitation spectrum consisted of two wide bands, which were located at about 268 and 324 nm. The emission spectrum, when excited at 324 nm, resulted in indigo light with a peak at about 442 nm.
© 2007 Elsevier Inc. All rights reserved.

Keywords: Calcium-chloro aluminate; Crystal structure; Powder diffraction; Rietveld refinement; Maximum entropy method; Electron density distribution; Luminescence

1. Introduction

Compounds of the type $Ca_{12}Al_{14}O_{32}X$ have been reported, where $X = 2F^-$ [1], $2Cl^-$ [2], O^{2-} [3–7] and $2OH^-$ [8]. All of these crystal structures are considered to be homeotypic to one another, belonging to the same space group $I\bar{4}3d$. For the compound with $X = 2F^-$, the crystal structure contained positional disordering of Ca sites and occupational disordering of F site [1]. The Ca sites are split into two positions, Ca(1) and Ca(2), with a separation of 0.05 nm. The interatomic distances are shorter for Ca(2)–F ($= 0.231$ nm) than for Ca(1)–F ($= 0.282$ nm), hence the F site is only occupied, with the occupancy of 1/3, when the Ca(2) position is also occupied.

The compound with $X = 2Cl^-$ ($Ca_{12}Al_{14}O_{32}Cl_2$) is one of the main constituents of a new type of Portland cement, termed "Eco-cement" [9]. This cement has been recently developed in order to solve the municipal waste problems caused by limited availability of landfill sites. The municipal waste incinerator ash is used as a part of the raw materials. Because the incinerator ash normally contains Cl components in relatively high concentrations, the resulting Eco-cement includes up to 20% of $Ca_{12}Al_{14}O_{32}Cl_2$ instead of $Ca_3Al_2O_6$, which is one of the main constitutes of normal Portland cement. The crystal structure of $Ca_{12}Al_{14}O_{32}Cl_2$ is, in spite of the importance in cement chemistry, still not elucidated so far. On the other hand, the crystal structure of $Ca_{12}[Al_{10.6}Si_{3.4}]O_{32}Cl_{5.4}$ has been determined by Feng et al. [10] using single-crystal X-ray diffraction method. In the structural model there are two distinct types of Al/Si sites, Al/Si(1) and Al/Si(2). The significantly shorter Al/Si(1)–O distances (average $= 0.1715$ nm) compared with Al/Si(2)–O (average $= 0.1762$ nm) can be related to the distribution of Si in the Al/Si(1) site [10]. The incorporation

*Corresponding author. Fax: +81 52 735 5289.
E-mail address: fukuda.koichiro@nitech.ac.jp (K. Fukuda).

of Si into Al sites led to an increase in Cl content to an extent that requires to maintain charge balance. The crystal structure is positionally ordered in that there is one Ca site.

The compound with $X = O^{2-}$ has recently received much attention as a room temperature-stable electride [11]. This material, when activated with Eu^{2+}, showed indigo-light luminescence with a peak wavelength of about 440 nm under UV excitation [12]. The excitation and emission spectra showed the characteristic broadband of the Eu^{2+} ion. Co-doping of Eu^{2+} and Nd^{3+} ions resulted in long afterglow phosphorescence.

Recent advances in modern crystal-structure analyses have enabled us to readily determine three-dimensional distribution of electron densities from X-ray powder diffraction (XRPD) data using the maximum-entropy method (MEM) [13]. However, the Rietveld [14] and MEM analyses are insufficient to derive charge densities because the observed structure factors, F_0(Rietveld), are biased toward the structural models. The subsequent MEM-based pattern fitting (MPF) method [15] reduces the bias as much as possible. Thus, the MEM and MPF analyses are alternately repeated (REMEDY cycle) until the reliability indices no longer decrease. Crystal structures are represented not by structural parameters but by electron densities in MPF.

In the present study, we have prepared the $Ca_{12}Al_{14}O_{32}Cl_2$ powder specimen to refine the crystal structure from XRPD data using the MEM/Rietveld and MPF methods. The crystal has been applied to a new host material for phosphors. We have reported the photoluminescence properties of $Ca_{12}Al_{14}O_{32}Cl_2$:Eu^{2+} to compare with those of $Ca_{12}Al_{14}O_{33}$:Eu^{2+}.

2. Experimental

2.1. Structure refinement

A specimen of $Ca_{12}Al_{14}O_{32}Cl_2$ for structural study was prepared from reagent-grade chemicals $CaCO_3$, Al_2O_3 and $CaCl_2 \cdot 2H_2O$. Well-mixed chemicals with Ca:Al:Cl = 6:7:1 in molar ratio were pressed into pellets (12 mm diameter and 3 mm thick), heated at 1273 K for 24 h, followed by quenching in air. Experimental XRPD intensities were collected at 298 K on a PANalytical X'Pert PRO Alpha-1 diffractometer equipped with a high-speed detector (X'Celerator) in the Bragg–Brentano geometry using monochromatized $CuK\alpha_1$ radiation (45 kV, 40 mA). Other experimental conditions were: continuous scan, 2θ range from 17.0032° to 148.4958°, total of 15738 datapoints, and total experimental time of 11.0 h. The divergence slit of 0.25° was employed to collect the quantitative profile intensities over the whole 2θ range.

2.2. Luminescence

A phosphor specimen with the formula $Ca_{11.76}Eu^{2+}_{0.24}Al_{14}O_{32}Cl_2$ was prepared by a solid-state reaction. Well-mixed chemicals of $CaCO_3$, Al_2O_3, $CaCl_2 \cdot 2H_2O$ and Eu_2O_3 were heated at 1423 K for 2 h in reducing atmosphere of N_2 (95 vol%) and H_2 (5 vol%), followed by cooling to ambient temperature by cutting furnace power. The XRPD intensities were collected on the diffractometer in a 2θ range from 17.00° to 80.00°. Excitation and emission spectra at 298 K were recorded with a Hitachi F-7000 fluorescence spectrometer.

3. Results and discussion

3.1. Structure refinement and description

Peak positions of the experimental diffraction pattern were first determined using the computer program PowderX [16]. The 2θ values of 40 observed peak positions were then used as input data to the automatic indexing program TREOR90 [17]. One cubic cell was found with satisfactory figures of merit $M_{20}/F_{20} = 65/69(0.004680,62)$ and $M_{40}/F_{40} = 58/59(0.003824,179)$ [18,19]. The derived unit-cell parameter of $a = 1.200779(9)$ nm could index all the observed reflections in the experimental diffraction pattern. The observed diffraction peaks showed systematic absences $h+k+l \neq 2n$ for hkl and $2h+l \neq 4n$ for hhl reflections, which are consistent with the space group $I\bar{4}3d$.

Initial structural parameters were taken from Feng et al. [10] giving the occupancy of Cl site, g(Cl), to be 1/3, corresponding to the chemical formula of $Ca_{12}Al_{14}O_{32}Cl_2$. The structural parameters were refined by the Rietveld method using the program RIETAN-FP [20]. A Legendre polynomial was fitted to background intensities with 12 adjustable parameters. The pseudo-Voigt function [21] was used to fit the experimental peak profiles. Isotropic atomic displacement parameters were initially assigned to all atoms. The refinement resulted in the reliability (R) indices [22] of $R_{wp} = 8.65\%$ ($S = 1.23$), $R_p = 6.19\%$, $R_B = 1.58\%$ and $R_F = 1.03\%$. We subsequently assigned anisotropic atomic displacement (U) parameters to obtain the lower R indices of $R_{wp} = 8.48\%$ ($S = 1.21$), $R_p = 6.05\%$, $R_B = 1.27\%$ and $R_F = 1.01\%$. The number of reflections employed were 372, and the number of refined parameters were 25 for the profile and 24 for the structure. The structure data were standardized using the computer program STRUCTURE TIDY [23], which was implemented in the program RIETAN-FP. The three-dimensional EDD and crystal-structure model were visualized using the software package VESTA [24]. Crystal data are given in Table 1, and the final positional and U parameters of atoms are given in Tables 2 and 3, respectively. A portion of the crystal structure is illustrated in Fig. 1.

The MPF method was subsequently applied in order to confirm the validity of the final structural model. After one REMEDY cycle, R_B and R_F decreased to 0.75% and 0.56%, respectively. The significant improvements of these R factors indicate that the crystal structure is represented more adequately with electron densities than with the structural model. The EDD determined by MPF (Fig. 2) is

Table 1
Crystal data and structure refinement for $Ca_{12}Al_{14}O_{32}Cl_2$

Chemical composition	$Ca_{12}Al_{14}O_{32}Cl_2$
Space group	$I\bar{4}3d$
a (nm)	1.200950(5)
V (nm^3)	1.73211(1)
Z	2
D_x (mg m^{-3})	2.74
Radiation and wavelength (nm)	$CuK\alpha_1$, 0.154059
2θ range (°)	$17.0032 \leqslant 2\theta \leqslant 148.4958$
Number of reflections	372
Number of refined profile parameters	25
Number of refined structural parameters	24
R_{wp} (S), R_p, R_B and R_F (Rietveld)	8.48% (1.21), 6.05%, 1.27%, 1.01%
R_B and R_F (MPF)	0.75%, 0.56%

Table 2
Atomic coordinates and equivalent isotropic displacement parameters for $Ca_{12}Al_{14}O_{32}Cl_2$

Atom	Position	g	x	y	z	$10^5 \times U$(eq)/ nm^2
O(1)	48e	1	0.03457(10)	0.44602(11)	0.14940(11)	10
Ca	24d	1	0.13961(5)	0	1/4	10
O(2)	16c	1	0.18427(11)	x	x	9
Al(1)	16c	1	0.01713(5)	x	x	7
Al(2)	12b	1	7/8	0	$\frac{1}{4}$	6
Cl	12a	1/3	3/8	0	$\frac{1}{4}$	23

U(eq) is defined as one-third of the trace of the orthogonalized U_{ij} tensor.

Table 3
Anisotropic displacement parameters ($10^5 \times U$/nm^2) for $Ca_{12}Al_{14}O_{32}Cl_2$

Atom	U_{11}	U_{22}	U_{33}	U_{12}	U_{13}	U_{23}
O(1)	7.7(7)	11.4(9)	10.0(7)	−2.7(6)	−3.3(5)	0.1(6)
Ca	11.4(4)	11.4(3)	6.1(3)	0	0	2.4(3)
O(2)	9.5(6)	U_{11}	U_{11}	−2.3(6)	U_{12}	U_{12}
Al(1)	6.9(2)	U_{11}	U_{11}	−0.1(2)	U_{12}	U_{12}
Al(2)	5.0(7)	6.6(4)	U_{22}	0	0	0
Cl	9(2)	29(1)	U_{22}	0	0	0

The anisotropic displacement factor exponent takes the form $-2\pi^2[h^2a^2U_{11} + k^2b^2U_{22} + l^2c^2U_{33} + 2hkabU_{12} + 2hlacU_{13} + 2klbcU_{23}]$.

explained satisfactorily by the present structural model (Fig. 1). We therefore concluded that, as long as the crystal structure is expressed by a structural model, the present structural model would be satisfactory. Observed, calculated, and difference XRPD patterns for the final MPF are plotted in Fig. 3.

Selected interatomic distances and bond angles, together with their standard deviations, are listed in Table 4. There are two Al sites in the structural model (Fig. 1), Al(1) and Al(2), in the ratio of 4:3. The Al(1) atom is coordinated to one O(2) atom and three O(1) atoms, with bond lengths ranging from 0.1723 to 0.1762 nm (the mean = 0.175 nm). The Al(2) atom is surrounded by four O(1) atoms (the
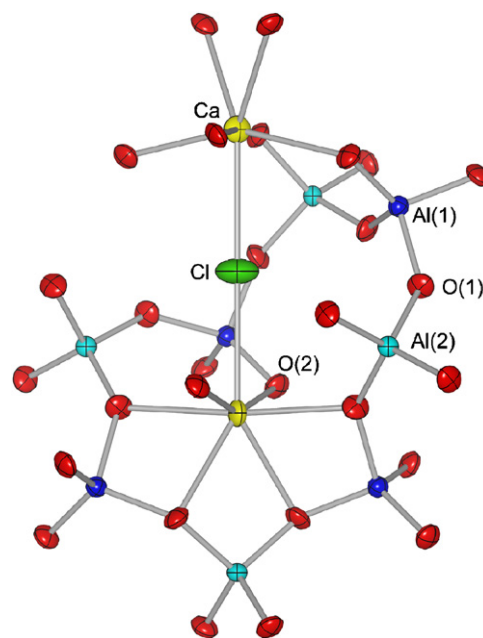

Fig. 1. A portion of the crystal structure of $Ca_{12}Al_{14}O_{32}Cl_2$ showing eight-membered AlO_4 rings and Ca–Cl–Ca unit. Numbering of atoms corresponds to that given in Table 2. Thermal ellipsoids represent 90% of probability.
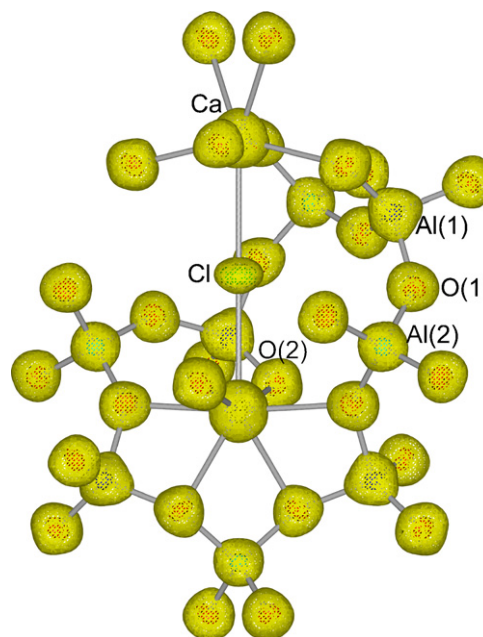

Fig. 2. Electron-density distribution determined by MPF in the same portion as that of Fig. 1. Isosurfaces expressed in wireframe style for an equidensity level of 0.002 nm^{-3}.

mean = 0.175 nm). Ionic radii of Al^{3+} in the four-fold coordination [$r(Al^{3+}) = 0.039$ nm and $r(O^{2-}) = 0.138$ nm] predict the interatomic distance of 0.177 nm for Al–O [25]. These values are in good agreement with the mean interatomic distances of Al(1)–O and Al(2)–O. The shared O(1) atoms connect alternating [Al(1)O$_4$] and [Al(2)O$_4$]
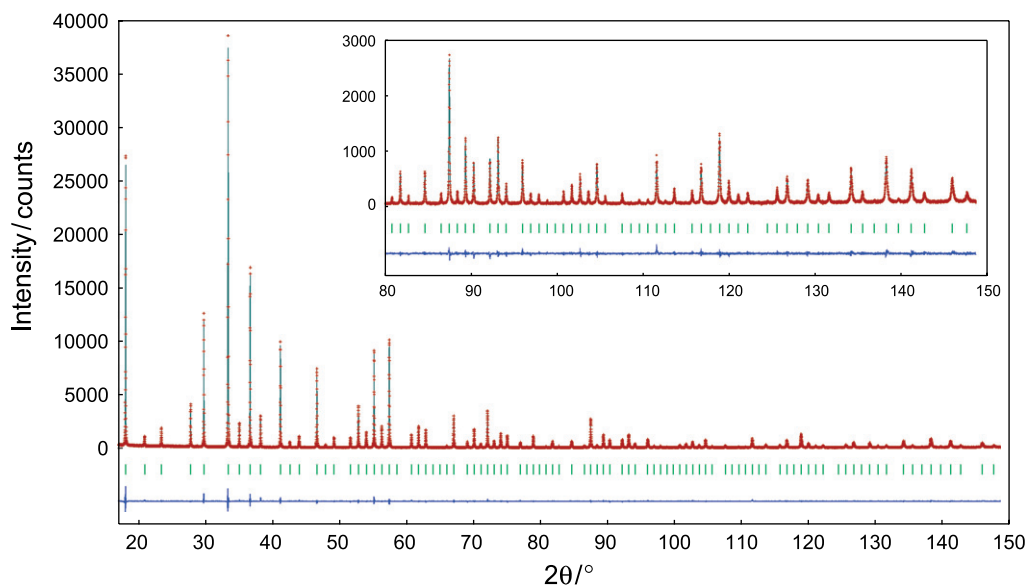
Fig. 3. Comparison of the experimental diffraction pattern of $Ca_{12}Al_{14}O_{32}Cl_2$ (symbol: $+$) with the corresponding calculated pattern (upper solid line) determined by MPF method. The difference curve is shown in the lower part of the diagram. Vertical bars indicate the positions of possible Bragg reflections.

Table 4
Selected interatomic distances (nm) and angles ($°$)

Ca–O(1)	$0.2393(1) \times 2$	Al(1)–O(2)	$0.1723(2)$	Al(2)–O(1)	$0.1749(1) \times 4$
Ca–O(2)	$0.2410(1) \times 2$	Al(1)–O(1)	$0.1762(1) \times 3$	O(1)–Al(2)–O(1)	$112.68(3) \times 4$
Ca–O(1)	$0.2501(1) \times 2$	O(1)–Al(1)–O(1)	$100.35(7) \times 3$		$103.24(7) \times 2$
Ca–Cl	$0.28269(6)$	O(1)–Al(1)–O(2)	$117.52(5) \times 3$		

tetrahedra to form boat-shaped eight-membered rings. The Ca atom is seven-fold coordinated by one Cl, four O(1) and two O(2) atoms. Linear units Ca–Cl–Ca lie on two-fold axis parallel to $\langle 100 \rangle$. This compound has been found to be isomorphous with $Ca_{12}Al_{10.6}Si_{3.4}O_{32}Cl_{5.4}$ [10]. The average Al/Si(1)–O distance of $Ca_{12}Al_{10.6}Si_{3.4}O_{32}Cl_{5.4}$ ($\langle Al/Si(1)–O \rangle = 0.1715$ nm) is appreciably shorter than the corresponding Al(1)–O distance of $Ca_{12}Al_{14}O_{32}Cl_2$ ($\langle Al(1)–O \rangle = 0.1752$ nm), which should be related to the preferential distribution of Si in the Al/Si(1) site.

3.2. Luminescence properties

The XRPD pattern of $Ca_{11.76}Eu_{0.24}^{2+}Al_{14}O_{32}Cl_2$ was very similar to that of $Ca_{12}Al_{14}O_{32}Cl_2$, indicating that the Eu^{2+} ions are homogeneously dispersed in the host crystal to form a single phase. The emission spectrum, when excited at a wavelength of the highest peak ($= 324$ nm) of the excitation spectrum, resulted in indigo light with a single peak at 442 nm (Fig. 4). The emission spectrum has a broadband character due to $4f$–$5d$ transitions of Eu^{2+} ion. The excitation spectrum shows two wide bands with their peaks at about 268 and 324 nm, which are most probably due to the crystal field splitting of the Eu^{2+} d orbitals. Both excitation and emission spectra were very similar to those of $Ca_{12}Al_{12}O_{33}:Eu^{2+}$ [12]. An attempt was made to

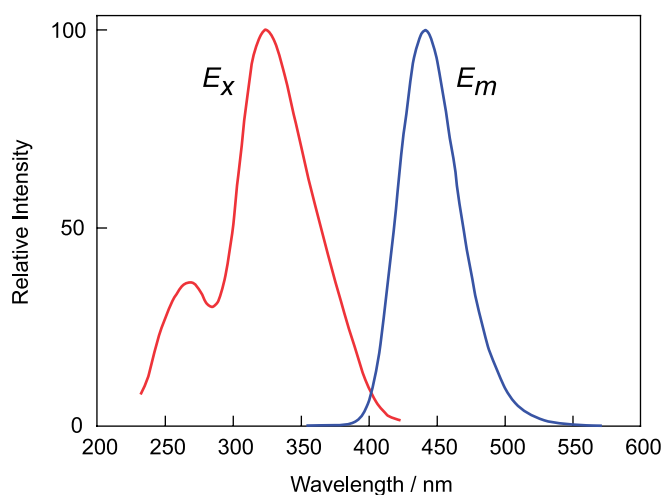Fig. 4. Emission (E_m) and excitation (E_x) spectra of $Ca_{11.76}Eu_{0.24}^{2+}$ $Al_{14}O_{32}Cl_2$ at 298 K.

synthesize the long afterglow phosphors by co-doping of Eu^{2+} and Nd^{3+} ions into the host $Ca_{12}Al_{14}O_{32}Cl_2$. However, the obtained phosphors $Ca_{12}Al_{14}O_{32}Cl_2$: Eu^{2+},Nd^{3+} did not show appreciable phosphorescence as compared with $Ca_{12}Al_{12}O_{33}:Eu^{2+},Nd^{3+}$ in a previous study [12].

4. Conclusion

We determined the crystal structure of $Ca_{12}Al_{14}O_{32}Cl_2$, which has a cubic unit cell with space group $I\bar{4}3d$. The validity of the structural model was verified by the electron density distribution, the structural bias of which was reduced as much as possible using the MPF method. This compound was isomorphous with $Ca_{12}Al_{10.6}Si_{3.4}O_{32}Cl_{5.4}$. The photoluminescence properties of $Ca_{12}Al_{14}O_{32}Cl_2:Eu^{2+}$ were very similar to those of $Ca_{12}Al_{12}O_{33}:Eu^{2+}$.

Acknowledgments

References

[1] P.P. Williams, Acta Crystallogr. B29 (1973) 1550–1551.
[2] C. Brisi, M.L. Borlera, Cemento 80 (1983) 155–164.
[3] H. Bartl, Neues Jahrb. Mineral Monatsh. 91 (1969) 404–413.
[4] W. Bussem, A. Eitel, Z. Kristallogr. 95 (1936) 175–188.
[5] J. Jeevaratnam, L.S. Dent Glasser, F.P. Glasser, Nature 194 (1962) 764–765.
[6] G. Hentschel, Neues Jahrb. Mineral Monatsh. 1 (1964) 22–29.
[7] H. Boysen, M. Lerch, A. Stys, A. Senyshyn, Acta Crystallogr. B63 (2007) 675–682.
[8] H. Bartl, Neues Jahrb. Mineral Monatsh. 91 (1969) 397–404.
[9] S. Yokoyama, Nyu Seramikkusu 11 (1998) 59–65.
[10] Q. Feng, F.P. Glasser, R.A. Howie, E.E. Lachowski, Acta Crystallogr. C 44 (1988) 589–592.
[11] S.-W. Kim, S. Matsuishi, M. Miyakawa, K. Hayashi, M. Hirano, H. Hosono, J. Mater. Sci. Mater. El. 18 (Suppl. 1) (2007) S5–S14.
[12] J. Zhang, Z. Zhang, T. Wang, W. Hao, Mater. Lett. 57 (2003) 4315–4318.
[13] M. Takata, E. Nishibori, M. Sakata, Z. Kristallogr. 216 (2001) 71–86.
[14] H.M. Rietveld, J. Appl. Crystallogr. 2 (1969) 65–71.
[15] F. Izumi, S. Kumazawa, T. Ikeda, W.-Z. Hu, A. Yamamoto, K. Oikawa, Mater. Sci. Forum 378–381 (2001) 59–64.
[16] C. Dong, J. Appl. Crystallogr. 32 (1999) 838.
[17] P.E. Werner, L. Eriksson, M. Westdahl, J. Appl. Crystallogr. 18 (1985) 367–370.
[18] P.M. de Wolff, J. Appl. Crystallogr. 1 (1968) 108–113.
[19] G.S. Smith, R.L. Snyder, J. Appl. Crystallogr. 12 (1979) 60–65.
[20] F. Izumi, T. Ikeda, Mater. Sci. Forum 321–324 (2000) 198–203.
[21] H. Toraya, J. Appl. Crystallogr. 23 (1990) 485–491.
[22] R.A. Young, in: R.A. Young (Ed.), The Rietveld Method, Oxford University Press, Oxford, UK, 1993, pp. 1–38.
[23] L.M. Gelato, E. Parthé, J. Appl. Crystallogr. 20 (1987) 139–143.
[24] F. Izumi, K. Momma, Solid State Phenom. 130 (2007) 15–20.
[25] R.D. Shannon, Acta Crystallogr. A32 (1976) 751–767.